Nitrogen and Water Adsorption in Aluminum Methylphosphonate α: A Molecular Simulation Study

Carmelo Herdes,[§] Zhi Lin,[⊥] Anabela Valente,[⊥] João A. P. Coutinho,[⊥] and Lourdes F. Vega*[,§]

Institut de Ciència de Materials de Barcelona, (ICMAB−CSIC), Consejo Superior de Investigaciones Científicas, Campus de la UAB, Bellaterra, 08193 Barcelona, Spain, and Centro de Investigação em Materiais Cerâmicos e Compósitos (CICECO), Department of Chemistry, University of Aveiro, 3810−193 Aveiro, Portugal

Received November 28, 2005. In Final Form: January 31, 2006

We present here Monte Carlo simulation and experimental results on the adsorption of nitrogen and water in aluminum methylphosphonate polymorph α (AlMePO-α). We have assumed a detailed atomic model for the material, using experimental information to construct the simulation cell. Nitrogen was modeled with two different approaches: as a simple Lennard-Jones (LJ) sphere with no charges, and as a diatomic molecule with charges explicitly included. Water was represented by the TIP4P model. Experimental adsorption isotherms were used to tune the proposed molecular model for the adsorbent. Simulated adsorption capacities were in agreement with the experimental results obtained for the studied systems. The influence of the surface model on the adsorption behavior was taken into account by considering different values of the surface methyl group size parameter. Our results corroborate the strong sensitivity of the simulation results to this parameter, as previously observed by Schumacher and co-workers. It is also observed that charged models are essential to accurately describe the low-pressure region of the adsorption isotherm, where the solid−fluid interaction rules the system behavior. However, a simple uncharged molecular model for nitrogen is able to describe the three loci arrangement at maximum loading. Experimental and simulation results presented here also confirm the low water affinity of AlMePO-α. These results enforce the application of this methodology to achieve quantitative predictions on similar systems, with the appropriate transferability of the molecular parameters.

I. Introduction

The study of micro- and mesoporous solids continues to be an area of active research, both from a fundamental point of view, and for their wide range of applications. Of particular relevance for several applications are materials with well-defined pores in the microporous region. It is well-known that the adsorption properties of porous materials strongly depend on both the chemical composition and the topology. Zeolites and similar microporous crystals present pore sizes in comparable dimensions with organic molecules, enabling selective adsorption on the basis of molecular size and shape. Nevertheless, the chemical properties of the adsorbent, such as the hydrophilic nature of the surface, may cause specific (usually, nondesired) interactions, with a direct influence over the adsorption process. Consequently, the challenge in the synthesis of these materials is to control not only the size and shape of the pores, but also the wettability of the micropores, among other chemical properties. Among these materials, we should mention the aluminum methylphosphonate polymorphs (AlMePO's)[1,2] and some other organic−inorganic hybrid framework materials, such as the metal−organic framework (MOF) and the inverted metal−organic framework (IMOF).[3] These hybrid materials present several potential applications in industry, some of them still unexplored. Maeda et al.[1,2] first reported the hybrid inorganic−organic materials AlMePO-β and AlMePO-α. Their aim was to design a porous system in which organic groups were part of the framework. They were able to control the size and shape of the pores and, in addition, tune their hydrophobic character, suiting attractive materials for molecular sieves, shape-selective catalysis, ion-exchanging, selective separation, and several others applications.

Since their inception, both polymorphs of AlMePO (α and β), prepared by different procedures, have been the subject of massive experimental and theoretical studies.[1,2,4−18] These studies have driven to well-characterized and reproducible crystal structures. Moreover, these solids are among the most thoroughly structurally characterized microporous, hybrid organic−inorganic materials,

* Corresponding author. E-mail: lvega@icmab.es.
§ Consejo Superior de Investigaciones Científicas, ICMAB-CSIC.
⊥ University of Aveiro.

(1) Maeda, K.; Akimoto, J.; Kiyozumi, Y.; Mizukami, F. *J. Chem. Soc., Chem. Commun.* **1995**, *10*, 1033.
(2) Maeda, K.; Akimoto, J.; Kiyosumi, Y.; Mizukami, F. *Angew. Chem., Int. Ed. Engl.* **1995**, *34*, 1199.
(3) Papaefstathiou, G. S.; MacGillivray, L. R. *Coord. Chem. Rev.* **2003**, *246*, 169.
(4) Rocha, J.; Lin, Z.; Fernandez, C.; Amoureux, J. P. *Chem. Commun.* **1996**, *22*, 2513.
(5) Maeda, K.; Hashiguchi, Y.; Kiyozumi, Y.; Mizukami, F. *Bull. Chem. Soc. Jpn.* **1997**, *70*, 345.
(6) Maeda, K.; Kiyozumi, Y.; Mizukami, F. *J. Phys. Chem. B* **1997**, *101*, 4402.
(7) Maeda, K.; Sasaki, A.; Watanabe, K.; Kiyozumi, Y.; Mizukami, F. *Chem. Lett.* **1997**, 9, 879.
(8) Carter, V. J.; Wright, P. A.; Gale, J. D.; Morris, R. E.; Sastre, E.; Perez-Pariente, J. *J. Mater. Chem.* **1997**, *7*, 2287.
(9) Brown, S. P.; Ashbrook, S. E.; Wimperis, S. *J. Phys. Chem. B* **1999**, *103*, 812.
(10) Carter, V. J.; Kujanpaa, J. P.; Riddell, F. G.; Wright, P. A.; Turner, J. F. C.; Catlow, C. R. A.; Knight, K. S. *Chem. Phys. Lett.* **1999**, *313*, 505.
(11) Maeda, K.; Mizukami, F. *Catal. Surv. Jpn.* **1999**, *3*, 119.
(12) Edgar, M.; Carter, V. J.; Tunstall, D. P.; Grewal, P.; Favre-Nicolin, V.; Cox, P. A.; Lightfoot, P.; Wright, P. A. *Chem. Commun.* **2002**, *8*, 808.
(13) Li, N.; Xiang, S. H. *J. Mater. Chem.* **2002**, *12*, 1397.
(14) Edgar, M.; Carter, V. J.; Grewal, P.; Sawers, L. J.; Sastre, E.; Tunstall, D. P.; Cox, P. A.; Lightfoot, P.; Wright, P. A. *Chem. Mater.* **2002**, *14*, 3432.
(15) Wu, Z. B.; Liu, Z. M.; Tian, P.; He, Y. L.; Xu, L.; Liu, X. M.; Bao, X. H.; Liu, X. C. *Microporous Mesoporous Mater.* **2003**, *62*, 61.
(16) Kimura, T. *Chem. Mat.* **2003**, *15*, 3742.
(17) Maeda, K. *Microporous Mesoporous Mater.* **2004**, *73*, 47.
(18) Grewal, P.; Radhamonyamma, N.; Gonzalez, J.; Wright, P. A.; Cox, P. A. *Recent Advances in the Science and Technology of Zeolites and Related Materials*; Proceedings of the 14th International Zeolite Conference, Cape Town, South Africa, April 25−30, 2004; van Steen, E., Callanan, L. H., Claeys, M., Eds.; Elsevier: Amsterdam, 2004; Vol. 154 (A,B,C), p 1777.

10.1021/la0532151 CCC: $33.50
Published on Web 03/01/2006

by means of single-crystal X-ray structural analysis in conjunction with nuclear magnetic resonance (NMR) spectroscopy (^{31}P, ^{13}C, and multiple-quantum magic angle spinning (MQMAS) ^{27}Al spectra);[4,6,9,10,15] thermogravimetric−differential thermal analysis (TG−DTA); IR; and transmission electron microscopy (TEM).[15] Adsorption isotherms have been used to calculate the pore diameter,[6] while water adsorption isotherms have been used to confirm the hydrophobic nature for both polymorphs.[6] The thermal transformation from polymorph β to α has been investigated by ^{27}Al MQMAS NMR,[9] while neutron powder diffraction and ^{2}H NMR spectroscopy have been used to examine the structure and rotational dynamics of CD_3 (deuterated methyl) groups.[10] The crystal structure was solved by a combination of computational energy minimization using density functional theory (DFT) with 1D MAS NMR and 2D 5Q MAS NMR spectroscopy and X-ray powder diffraction.[12,14] Finally, Monte Carlo/simulated annealing simulations highlighted the templating role of 1,4-dioxane in the formation of AlMePO-β.[18]

One should note that, despite all the experimental efforts done in this field, the theoretical study of these materials still remains a challenge, mostly unexplored. The recent work of Schumacher and co-workers[19] is the first molecular simulation study about the adsorption of gases in the two AlMePO polymorphs. They used grand canonical Monte Carlo[20] (GCMC) simulations to mimic the adsorption of nitrogen and carbon dioxide on these materials. In this pioneering work, they proposed a model for the materials in which the position of the atoms forming the solid was determined by a combination of neutron diffraction experiments and ^{2}H NMR calculations (see the original article for details). They found that small differences between the AlMePO-α and AlMePO-β adsorbent structures have strong influences on their respective adsorption behaviors. These results promote the use of these materials for highly selective adsorption separations. The model system of Schumacher et al.[19] was able to capture some important features of the real adsorbent, being a step forward in obtaining molecular models of these materials for predictive purposes. However, the simulations performed using these models, as they are, are extraordinarily dependent upon the molecular size parameters used; this fact promotes the search for more transferable potential parameters and/or the testing of the available ones with different systems to provide reliable tools for predictive purposes.

The objective of the present study is twofold: (1) to get some insight into the physicochemical characteristics of AlMePO-α by means of molecular simulations, and (2) to provide/test simulation tools to accurately describe the adsorption behavior of nitrogen and water on this material. Our final goal is to set up a reliable framework to investigate future applications of these microporous crystals in a predictive manner.[21]

The rest of the paper is organized as follows: We first present both the experimental and the modeling methodology used, including details on the synthesis protocol, the adsorption equipment, the molecular models used for the fluids and the material, and the relevance of the electrostatic contribution. The results and discussion are presented in section 3, where we show single adsorption isotherms of nitrogen and water, as obtained experimentally and with different molecular models. We also discuss the arrangement of molecules inside the pores, depending on the studied conditions. Finally, we summarize the main conclusions in the last section.

II. Methodology

To control the whole cycle, synthesis, characterization, modeling, and applications, we obtained the experimental data used to validate the molecular models. This also includes the synthesis of the material.

II.1. Experimental Section. AlMePO-α was synthesized based on the reported procedure.[2] Crystals were obtained from an unstirred aqueous mixture ($Al/P/H_2O$ = 1:1.7:44) of methylphosphonic acid (Aldrich, 98 wt %) and pseudo-boehemite powder (PURAL SB from Condea; 67.01 wt % Al_2O_3, 32.99 wt % H_2O). The mixture was hydrothermally treated at 433 K for 48 h without stirring under an autogenous pressure using an autoclave with a Teflon sleeve. The air-dried product gave an approximate composition of $Al_2(CH_3PO_3)_3\ nH_2O$ ($n = 0-1.5$) from elemental analyses. Since this procedure also results easily in AlMePO-β, the AlMePO-α structure for each sample was confirmed by X-ray diffraction and ^{31}P and ^{27}Al MAS NMR spectra.

The structural characterization of the material was performed by adsorption of two different fluids: nitrogen (at 77 K) and water (at 298 K). Adsorption isotherms were measured using a gravimetric adsorption apparatus equipped with a CI Electronics MK2-M5 microbalance. Adsorbate−adsorbent equilibrium of each data point was monitored using CI Electronics Labweigh software, and the pressure was monitored using an Edwards Barocel pressure sensor. The solids were outgassed at 543 K overnight to a residual pressure of $\sim 10^{-4}$ mbar and then cooled to the desired temperature for adsorption measurements. The values of specific surface area and specific total pore volume were calculated from the data of nitrogen adsorption at 77 K, knowing the projection area of a nitrogen molecule to be 0.162 nm^2/molecule and using a liquid density of N_2 at 77 K of 0.8081 g cm^{-3}. Dissolved air was removed from distilled−deionized water using freeze−pump−thaw cycles before use. X-ray diffraction studies were run over the as-synthesized material before and after the adsorption process on a Philips X'pert MPD diffractometer using Cu Kα radiation. ^{31}P and ^{27}Al MAS NMR spectra were recorded at 162.0 and 104.3 MHz, respectively, on an Avance (9.4 T, wide-bore) Bruker spectrometer.

II.2. Molecular Models. *Adsorbent Material Model.* Because of the well-described crystallographic information available about AlMePO-α, we assumed a detailed atomic model for the material. As a first approach to the system, the individual atoms forming the solid were represented by single Lennard-Jones (LJ) spheres; the required properties of each atom to describe the potential energy of the adsorbate are the LJ collision diameter σ and the well depth ϵ. In a second step of complexity, in addition to the LJ sites, a Coulombic point charge q was implemented for each atom. These intermolecular parameter values, provided in Table 1, were selected from the work of Schumacher et al.[19] (and references there in). We also performed a tune-fitting procedure to fit the results of our simulations with our experimental nitrogen adsorption isotherm on AlMePO-α, searching for quantitative agreement with experimental data, and thereby improving the results of Schumacher and co-workers.

The AlMePO-α model material was created from the crystallographic unit cell identified by Maeda et al.,[2] in the trigonal space group $P31c$ with a = 13.9949(13) Å and c = 8.5311(16) Å. The structure is based on a three-dimensional net in which

(19) Schumacher, C.; Gonzalez, J.; Wright, P. A.; Seaton, N. A. *Phys. Chem. Chem. Phys.* **2005**, *7*, 2351.

(20) Allen, M. P.; Tildesley, D. J. *Computer Simulation of Liquids*, 2nd ed.; Clarendon Press: Oxford, 1989.

(21) Herdes, C.; Lin, Z.; Valente, A.; Coutinho, J. A. P.; Vega, L. F. To be submitted for publication, 2006.

Table 1. Molecular Model Parameters

	σ (nm)	ϵ/k (K)	q (e_0)
nitrogen (a)	0.3615	101.5	
nitrogen (b)[a]	0.331	36.0	−0.482
	water[b]		
oxygen	0.315	78.0	
hydrogen			+0.52
	AlMePO-α[c]		
Al			+2.19
P			+2.30
O	0.2655	128.13	−1.15
CH_3	0.3500	120.15	-
C			−1.21
H			+0.30

[a] N−N interatomic distance is 0.11 nm. A center charge of $+0.964e_0$ is assigned for neutrality. [b] A center-of-mass charge of $-1.04e_0$ is assigned for neutrality. [c] Values selected from the work of Schumacher et al.[19]

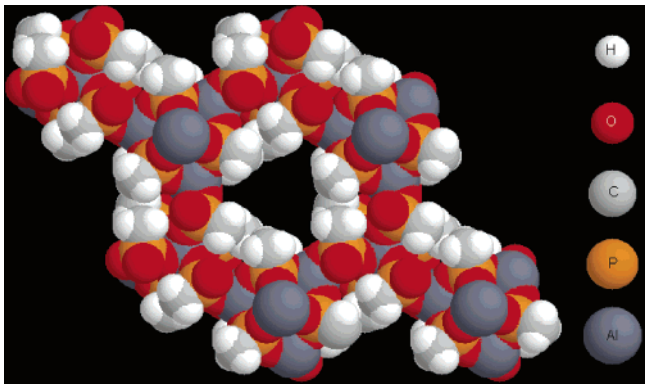

Figure 1. Atomistic description of AlMePO-α based on crystallographic information. The van der Waals radii of 2.05, 1.80, 1.70, 1.52, and 1.2 Å for Al, P, C, O, and H, respectively, were used to draw the figure (right). This hexagonal cell contains four parallel channels in the *z* direction.

aluminates and methylphosphonates alternate as in AlPO's.[22−24] AlPO's are generally composed of only four-connected nets, while AlMePO-α includes not only four-coordinates, but also topologically three-connected phosphorus with terminal methyl groups. To compensate the framework charge, one of the three oxygen atoms in each CH_3PO_3 group is bonded to a six-coordinate aluminum atom; the other two oxygen atoms are bonded to four-coordinate aluminum atoms (see Figure 1). The most remarkable feature of AlMePO-α is the existence of one-dimensional channels running parallel to the *c* axis with all the methyl groups pointing toward the center of the channels.[2]

The simulation cell (shown in Figure 1) comprises 96 aluminum atoms, 432 oxygen atoms, 144 carbon atoms, 144 phosphorus atoms, and 432 hydrogen atoms. In this approach, the methyl groups were modeled as single LJ spheres, since the carbon and hydrogen positions are relevant just for the charge localization in electrostatic calculations. The periodic hexagonal simulation cells for AlMePO-α consist of a $2 \times 2 \times 3$ crystallographic unit cell, containing four unidimensional channels.

Adsorbate Fluids Models. Nitrogen was modeled using two different approaches: (a) a simple model with no charges and (b) a more sophisticated model that is diatomic with charges explicitly considered. These two models were chosen to determine the influence of the electrostatic contributions on the internal energy in the adsorption process.

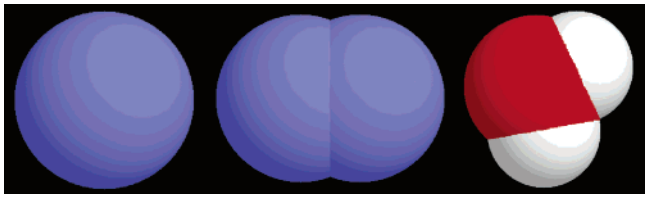

Figure 2. A sketch of the LJ and TraPPE models for nitrogen and the TIP4P model of water (charges are not represented here).

In model a, the simple model, nitrogen molecules were represented by single LJ spheres, with parameters $\sigma_{ff} = 0.3615$ nm and $\epsilon_{ff}/k = 101.5$ K, with k being Boltzmann's constant. Ravikovitch et al.[25] chose those fluid−fluid parameters to fit with the bulk properties of nitrogen, including liquid−gas surface tension and reference adsorption isotherms on nonporous substrates. No point charges were placed in this model, the neglecting of the quadrupole of the nitrogen being, a priori, a shortfall of the model. However, our intention was to check whether this simple model was able to describe the adsorption behavior of the experimental system.

Model b, the refined model, was constructed following the work by Potoff and Siepmann.[26] We used the transferable potential for phase equilibria (TraPPE) force field, with two LJ sites described by $\sigma_{ff} = 0.331$ nm and $\epsilon_{ff}/k = 36.0$ K, and a linear array of three charges distributed at the atom position and at the center of the nitrogen−nitrogen bond (the N−N interatomic distance is 0.11 nm). The charges were $q_N = -0.482e_0$ in each nitrogen atom, and the center charge was $q_{N-N} = +0.964e_0$. This representation of the molecular charge distribution on nitrogen mimics the experimentally measured quadrupole moment (which is commonly treated as an adjustable parameter in other molecular models).

The force field chosen to model water was taken from Jorgensen et al.[27] The so-called TIP4P potential uses four interaction sites in each water molecule, that is, three charged sites and a separated center-of-mass coinciding with the oxygen center. This results in nine electrostatic terms for the water−water interaction. The oxygen is an uncharged LJ site described by $\sigma_0 = 0.315$ nm and $\epsilon_0/k = 78.0$ K. The charges are $q_H = +0.52e_0$ in each hydrogen atom, and the center-of-mass charge is $q_M = -1.04e_0$.

The standard Lorentz−Berthelot rules were used to calculate the interaction between different species (and with the surfaces). Figure 2 depicts the above-described models for adsorbate molecules, where charges are not explicitly represented. Short-range interactions between two sites (at different molecules) were calculated using the common 12−6 LJ potential function. The calculation of the long-range interactions is explained in the next subsection.

II.3. Simulation Details. The electrostatic contribution to the internal energy was calculated using the Ewald summation.[28−32] The real space cutoff used was half the smallest width of the

(22) Wilson, S. T.; Lok, B. M.; Messina, C. A.; Cannan, T. R.; Flanigen, E. M. *J. Am. Chem. Soc.* **1982**, *104*, 1146.
(23) Flanigen, E. M.; Lok, B. M.; Patton, R. L.; Wilson, S. T. *New Developments in Zeolite Science and Technology*; Murakami, Y., Iijima, A., Ward, J. W., Eds.; Elsevier: Amsterdam, 1986; p 103.
(24) Bennett, J. M.; Dytrych, W. J.; Pluth, J. J.; Richardson, J. W.; Smith, J. W., Jr. *Zeolites* **1986**, *6*, 349.
(25) Ravikovitch, P. I.; Vishnyakov, A.; Neimark, A. V. *Phys. Rev. E* **2001**, *64*, 011602.
(26) Potoff, J. J.; Siepmann, J. I. *AIChE J.* **2001**, *47*, 1676.
(27) Jorgensen, W. L. *J. Chem. Phys.* **1982**, *77*, 4156.
(28) Frenkel, D.; Smit, B. *Understanding Molecular Simulation from Algorithms to Applications*; Academic Press: London, 1996.
(29) Ewald, P. P. *Ann. Phys.* **1920**, *64*, 253.
(30) Gregg, S. J.; Sing, K. S. W. *Adsorption, Surface Area and Porosity*; Academic Press: New York, 1982.
(31) Smith, W.; Forester, T. R. *The DLPOLY 2 User Manual*, version 2.13; CCLRC, Daresbury Laboratory: Cheshire, U.K., 2001.
(32) Smith, W.; Fincham, D. *Mol. Simul.* **1993**, *10*, 67.

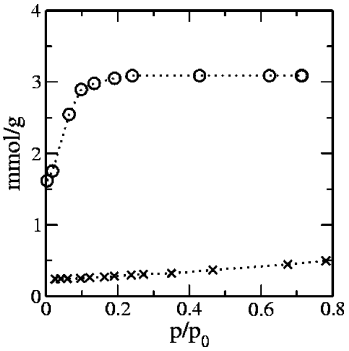

Figure 3. (○) Experimental nitrogen adsorption isotherm at 77 K and (×) experimental water adsorption isotherm at 298 K. The doted lines are guides for the eye.

simulation box; thus only the nearest image interacting charges had to be taken into account. The convergence parameter was set to 0.27 (from ref 19), and the number of *k*-vectors in the Fourier space sum was 1330. Test runs ensured that the Ewald sum converged sufficiently not to affect the outcome of the simulations. We took advantage of the fact that the positions of the atoms of the model adsorbent, including the methyl groups, were fixed during the whole simulation.[19] This implies that the solid−solid interactions do not affect the calculations, since they cancel out when energetically comparing simulated configurations; hence, only solid−fluid and fluid−fluid interactions were calculated along the simulations. To save computation time, we "turned on" the electrostatic calculation when the system had reached an "equilibrated state" by just computing the internal energy with simple LJ interactions (short-range contribution) in the equilibration period. We checked that this does not affect the final results obtained in the calculations, in comparison with selected simulations performed with electrostatic contributions from the initial state.

We obtained the individual adsorption isotherms by GCMC[20] simulations. In GCMC, the temperature, *T*, the volume pore, *V*, and the chemical potential, μ, are kept fixed. The number of molecules is thus allowed to vary, being that the average is the relevant quantity of interest. For convenience, to obtain the adsorption isotherm, we ran simulations at different values of the activity, ξ, defined as

$$\xi = \frac{\exp(\mu/kT)}{\Lambda^3} \tag{1}$$

where Λ is the de Broglie wavelength, which includes contributions from translational degrees of freedom; μ, *k*, and *T* were defined previously.

The usual magnitudes for representing adsorption data are the amount of fluid adsorbed in the pore versus the relative pressure p/p_0 in the bulk phase; here, p_0 is the bulk saturation pressure of each pure fluid. We used two different expressions to relate pressures with activities: (1) an "ideal" relationship $p/p_0 = \xi/\xi_0$, which implies that the bulk phase in thermodynamic equilibrium with the pore presents an ideal behavior,[33] and (2) the virial equation of state in terms of activity:[34]

$$p/p_0 = \frac{2\xi\xi_0{}^2 + (\rho_0 - \xi_0)\xi^2}{(\rho_0 + \xi_0)\xi_0{}^2} \tag{2}$$

where ξ_0 and ρ_0 are the activity and density of the saturation state

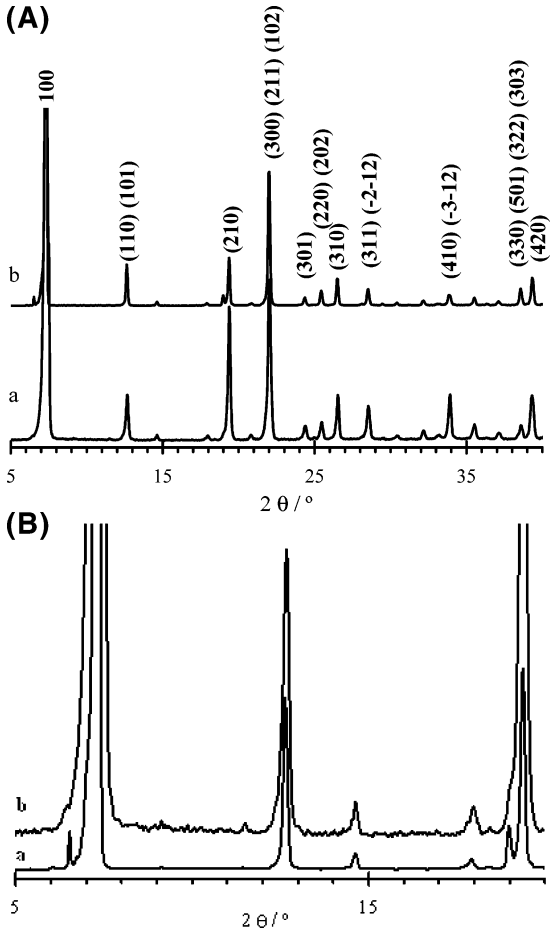

Figure 4. X-ray diffractograms of AlMePO-α before (a) and after (b) the nitrogen adsorption/desorption process. (A) The diffractograms showing the crystallographic indexes of the diffraction peaks. (B) Enlarged view of the diffractograms depicting the shoulders in the pattern of the sample before the adsorption experiments. See text for details.

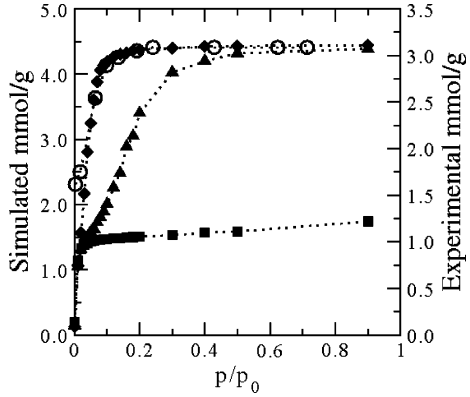

Figure 5. Nitrogen adsorption isotherm at 77 K: experimental (○) and simulated results using different values of σ_{CH3}, 0.350 nm (◆), 0.361 nm (▲), and 0.375 nm (■). The doted lines are guides for the eye.

point of the pure fluid at the needed temperature, respectively. The activity of the saturation state can be obtained either by an equation of state or by simulations of the same fluid, with the same model, in the bulk. The second approach was used in this work. The chosen state points for the reduction of activities to pressures were the saturation point of pure nitrogen at 77 K,

(33) Herdes, C.; Santos, M. A.; Medina, F.; Vega, L. F. *Langmuir* **2005**, *21*, 8733.

(34) Hansen, J.-P.; McDonald, I. R. *Theory of Simple Liquids*, 2nd ed.; Academic Press: London, 1986.

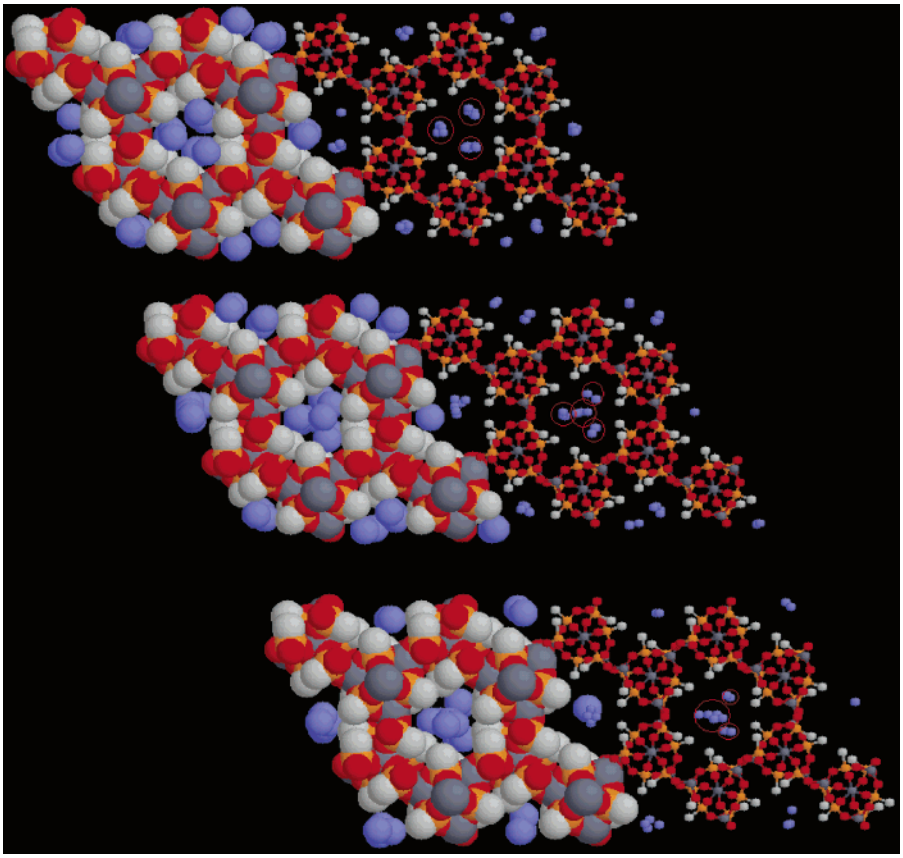

Figure 6. Snapshots showing the influence of increasing σ_{CH3}: from top to bottom, 0.350, 0.361, and 0.375 nm. The van der Waals radii of 2.05, 1.80, 1.70, 1.52, and 1.2 Å for Al, P, C, O, and H, respectively, were used to draw the figure (left). The ball-and-stick representation was used on the right-hand side for clarity. Red circles denote the preferential loci for nitrogen molecules inside the pores.

found to occur at $\xi_{N0} = 8.222 \times 10^{-2}$ nm^{-3} and $\rho_0 = 1.416 \times 10^{-1}$ mol/L for both models, and that of pure water at 298 K, corresponding to $\xi_{W0} = 8.698 \times 10^{-4}$ nm^{-3} and $\rho_0 = 1.693 \times 10^{-3}$ mol/L, as obtained from bulk GCMC simulations. We observed that there are no appreciable differences between the pressures obtained with either expression for nitrogen; however, the second expression (eq 2) is more appropriate for water, compared with the more accurate results obtained from more refined equations of state.[35]

Almost all simulation runs required 5×10^7 configurations to reach the equilibrium (first neglecting electrostatic contributions). Additional 1.5×10^8 configurations were generated, accounting for both short and long-range interactions. At some conditions, longer runs were needed to accomplish the equilibrium conditions. Average properties were calculated over blocks with 5×10^5 configurations once the equilibrium was reached. The fluid−fluid potential was cut at $r_c = 6\sigma_{ff}$, as recommended in ref 36.

To compare with experimental data, the excess pore fluid density was calculated as

$$\langle \rho_{exc} \rangle = \frac{\langle N \rangle}{V} - \rho_{bulk} \qquad (3)$$

where $\langle N \rangle$ is the mean number of molecules inside the pore, ρ_{bulk} is the bulk density value under the same conditions, calculated using the GCMC bulk method explained above, and V is the volume of the model pore.

(35) Llovell, F.; Pàmies, J. C.; Vega, L. F. *J. Chem. Phys.* **2004**, *121*, 10715.
(36) Duque, D.; Vega, L. F. *J. Chem. Phys.* **2004**, *121*, 8611.

III. Results and Discussion

Figure 3 shows the experimental nitrogen adsorption isotherm at 77 K in AlMePO-α. The nitrogen adsorption exhibits a type I isotherm according to the IUPAC classification,[30] which is the typical form for microporous solids (pore diameter < 2 nm). The material has a specific Langmuir area of 324 m^2/g and a total pore volume of 0.11 cm^3/g (calculated using Gurvitsch's rule). The maximum nitrogen loading was found to be 3.1 mmol/g.

A frequent drawback when removing organic traces in common molecular sieves is the high water adsorption capacity of these materials (referred to as hydrophilic behavior). Consequently, the efficiency in this kind of process separation is diminished when the environmental relative humidity increases. The water adsorption capacity of AlMePO-α at 298 K is approximately 85% less than the nitrogen adsorption capacity at 77 K (estimated at relative pressure $p/p_0 \approx 0.8$), as is depicted in Figure 3. These results show that AlMePO-α has a low affinity to adsorb highly polar molecules because of the methyl groups located on the surface, which confers a hydrophobic nature to the material.

To check the effect of the fluid adsorption on the material, we performed X-ray diffractograms before and after the nitrogen adsorption/desorption experiments. Results are presented in Figure 4, where the crystallographic indexes of the diffraction peaks are also included. The patterns before and after the adsorption process are very similar. There are only some small differences in the intensity of some reflections, attributed to orientation effects of large crystals. This can be better observed in an expansion of the powder pattern, shown in Figure 4B. It is seen that the shoulders were also present in the pattern of the sample before the adsorption experiments. Hence we can ensure that the crystalline structure of the material remains along this process.

Next we present the simulation results obtained with the procedure outlined in the previous section. It is important to point out that, when a straight comparison was made, the values of the nitrogen and water experimental adsorption isotherms were usually lower than those of the simulated adsorption isotherms. This may be due to the fact that the synthesized material contains pore defects and inaccessible pores (to one or both fluids), which effectively decrease the porosity, while the simulated material has a perfect crystalline structure. It can also be due to the way in which GCMC simulations are performed: molecules are created inside the pores in a random manner, and the creation is accepted with energetic arguments, but nothing is considered about the diffusion and/or pore-blocking effects inside the pores. This may promote simulated pore intakes greater than those obtained experimentally. To match the real porosity, a scale factor has been calculated, as the ratio between the experimental and the simulated adsorption; this factor should be in the range of 0−1.[19] A close value to unity represents a more crystalline structure in the real material, in the way considered in ref 19. Throughout this article comparative figures containing experimental and simulated adsorption results are represented with two *y*-axes, the left one corresponding to the simulated results, and the right one corresponding to experimental data.

The σ_{CH3} value reported in the anisotropic united atoms force field (AUA-FF),[37] is 0.36072 nm. This value represents the diameter of the methyl groups attached to the surface. Schumacher et al.[19] showed that the uptake of nitrogen is very sensitive to this parameter for the α-polymorph, while no significant changes were observed for the β-polymorph. We have further investigated this issue, performing simulations at three different values. The results are presented in Figure 5. Here, the three σ_{CH3} values selected were 0.361, 0375, and 0.350 nm. These three values correspond to the AUA-FF value (0.361 nm), a higher value, and a lower value, respectively. Nitrogen molecules were simulated using model a, the simple LJ model. As can be seen in Figure 5, the lowest σ_{CH3} value studied, 0.350 nm, gives an IUPAC type I isotherm[30] close to experimental values, with a scale factor of 0.70, calculated at maximum loading (which implies that the quality of the synthesized material is high). An increment in the σ_{CH3} value, up to the reported AUA-FF value[37] of 0.361 nm, results in a pore filling at higher pressures; besides that, an additional step appears at lower pressures. The adsorption isotherm with the highest σ_{CH3} studied, 0.375 nm, presents a type I behavior, but with half the experimental adsorption maximum loading.

A clear advantage of the use of molecular simulations to investigate the behavior of these systems is that the simulations provide the location of all atoms for any configuration. Snapshots of some configurations can provide remarkable insight into the understanding of what happens inside the model pores of the material when the methyl group's collision diameter is changed. The results for selected configurations are presented in Figure 6. The snapshots were taken at the maximum loading pressure. In these $x-y$ projections, it is clear that, when the value of σ_{CH3} is increased, nitrogen molecules are forced to pass from a three loci array (on the vertexes of the triangular pore channel) to a single rod (in the middle of the pore). Hence, the differences in adsorption are mainly due to steric effects, with the methyl group size being the most relevant parameter.

A closer look into the lower pressure region in Figure 5 shows that, in fact, model a is unable to capture the initial trend of the experimental system, probably because of the absence of

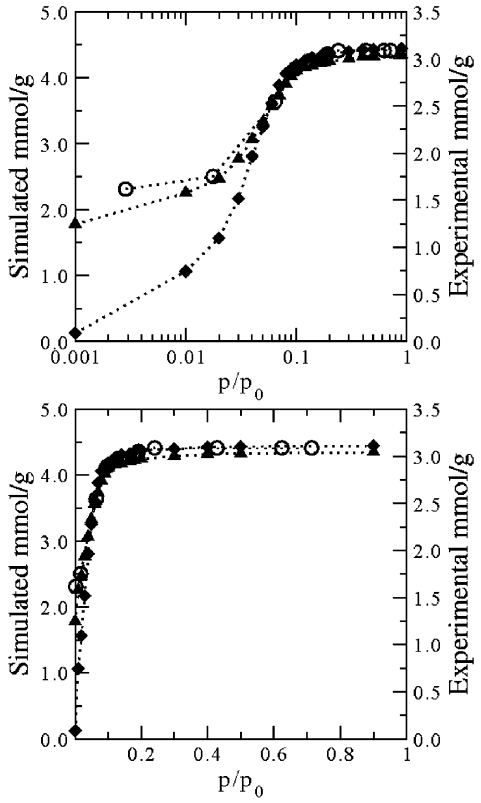

Figure 7. Nitrogen adsorption isotherm at 77 K: experimental (○) and simulated results using model a (▲) and model b (◆), with the same σ_{CH3} value of 0.350 nm. The relative pressures are represented in log-scale at the top and in linear-scale at the bottom. The dotted lines are guides for the eye.

electrostatic interactions in this model. In Figure 7, we present the comparison between the experimental and the simulated nitrogen adsorption isotherm on AlMePO-α for the two nitrogen models under study, with a σ_{CH3} value of 0.350 nm. Model b, with the Coulombic points charge and the evaluation of the electrostatic contribution to the energy, improves the description of the adsorption at lower pressures, and is in better agreement with the experimental data. The impact in the upper pressure region is not significant, and the scale factor remains approximately 0.7.

Comparative snapshots for maximum nitrogen loading using models a and b, referenced to the highest pressure of Figure 7, are presented in Figure 8. Both projections show equivalent molecule positions, reassuring the presence of the preferential three loci on the corner of the pore. Schumacher et al.[19] studied how regular the molecular arrangement is at maximum loading using model b and obtained the distribution of angles between the axis of the adsorbed molecules and the axis of the pore channels. They found that the steric compatibility between the adsorbent and the nitrogen molecules causes these stable configurations, ruling the shape of the adsorption isotherm.

It is important to mention that, although the differences among the three values of the methyl group size parameter seem to be small, they are not insignificant; note that this value greatly affects the available volume of the pore (as observed in Figure 6). Our results indicate that the AUA-FF value is not the best for these simulations. However, further investigations with other fluids should be done before a more definitive conclusion can be extracted about the optimum value. Moreover, the AUA-FF model provides excellent initial guess values for a tune-fitting procedure as the one used here.

(37) Ungerer, P.; Beauvais, C.; Delhommelle, J.; Boutin, A.; Rousseau, B.; Fuchs, A. H. *J. Chem. Phys.* **2000**, *112*, 5499.

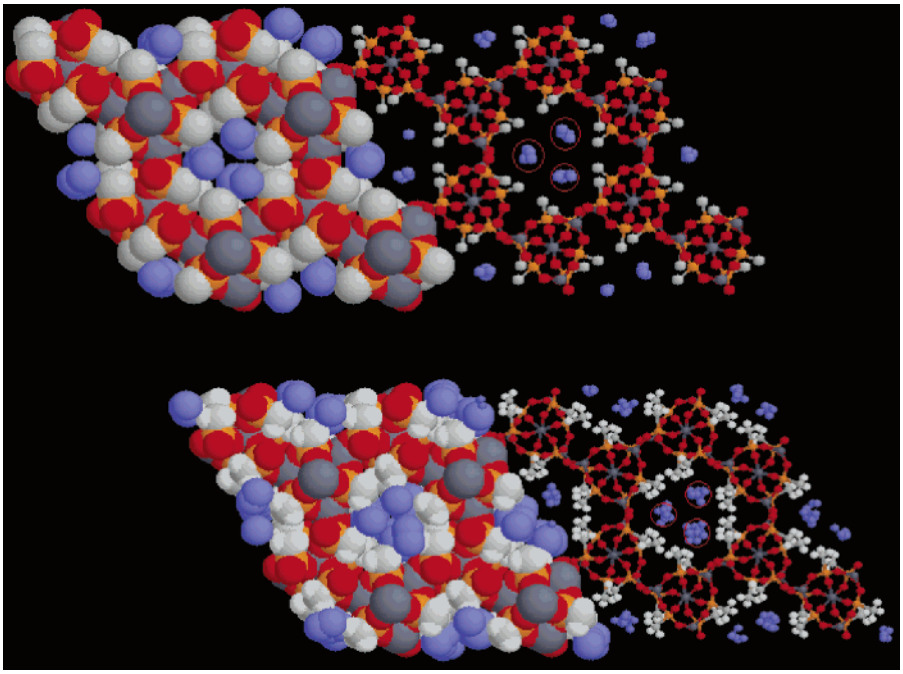

Figure 8. Comparative snapshots for maximum nitrogen loading using models a and b, referenced to the highest pressure of Figure 7. The symbols are the same as those in Figure 6.

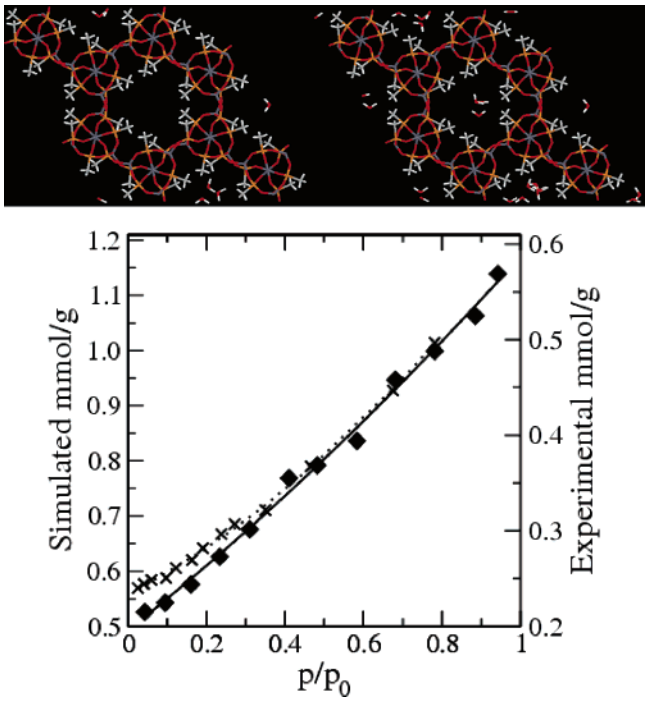

Figure 9. Water adsorption isotherm at 298 K: experimental (×) and simulated results (◆) with $\sigma_{CH3} = 0.350$ nm. The full and dotted lines are quadratic trend lines over the simulated and experimental values, respectively. The snapshots correspond to the minimum and maximum water loadings.

To check the predictive capability of the material model, we used it to calculate the adsorption of water at 298 K. The methyl group's diameter σ_{CH3} of the material had the same value as that in the nitrogen−AlMePO-α system, that is, 0.350 nm. This is a very challenging case, since the material model parameters, fitted to the adsorption of nitrogen, would be used to predict (with no fitting) the adsorption of a clearly nonideal fluid such as water. The simulated results are compared with the experimental data in Figure 9. Equation 2 was used to relate the activity with the pressure along the curve. An excellent overall agreement is observed in the range of pressures considered. A scale factor of 0.5 was used to match the simulated adsorption isotherm of water in AlMePO-α with the experimental behavior. The difference with the 0.7 scale factor used for nitrogen adsorption can be due to an "artifact" of the simulations performed with the GCMC method: note that, in this method, molecules appear inside the pore in a somehow artificial mode, since they are created randomly, while some of these locations may be forbidden in experimental cases due to diffusion problems and/or pore-blocking effects. Both problems are more acute for water adsorption than for nitrogen adsorption. It should also be noted that the methyl group parameters were fitted for nitrogen, whereas they are used here in a predictive manner; this is of special importance in the low-pressure adsorption regime, where the solid−fluid interaction is more relevant.

Caution should be taken when interpreting these results for further applications. AlMePO-α was found to be unstable in liquid water, while the location of the atoms forming our model materials are fixed along the simulations, as explained above. Consequently, if any structural modification on the real crystal occurs, especially with the increase in the relative pressure of water, these material alterations will not be reflected in our simulated water adsorption isotherm. The water simulations presented here are of clear relevance for further applications of the material, especially for separation purposes, a subject of future work.[21]

IV. Conclusions

The objective of this work was to develop and tune a molecular simulation model of the AlMePO-α material to be used in future applications. The material was synthesized and characterized in our laboratory. GCMC simulations were used to obtain the adsorption isotherm of nitrogen, with two molecular models, and of water.

These simulations allowed us to corroborate the strong sensitivity of the simulation results to the LJ diameter of methyl groups, as previously observed by Schumacher and co-workers.[19] We have proved that the charged models are essential to accurately

describe the low-pressure region of the adsorption isotherm, where the solid−fluid interaction rules the system behavior. However, a simple uncharged molecular model for nitrogen is able to describe the three loci arrangement at maximum loading.

Our simulated adsorption results show that the model used for AlMePO-α has a low affinity for adsorbing highly polar molecules, such as water molecules. This was expected, and it is due to the presence of the methyl groups located on the surface, which mimics the hydrophobic nature of the real material. The water adsorption simulations have proved the transferability of the model material parameter for predicting the adsorption behavior of other fluids in this material, including mixtures.

Acknowledgment. The authors thank the financial support received from the Spanish Government (projects HP2002-0089, CTQ2004-05985-C02-01, and CTQ2005-00296/PPQ). C.H. acknowledges a grant from MATGAS A.I.E.

LA0532151